ELSEVIER

Journal of Chromatography A, 724 (1996) 255–264

JOURNAL OF CHROMATOGRAPHY A

Time-integrated spectra from a flame photometric detector[1]

Hameraj Singh, Brian Millier, Walter A. Aue*

Department of Chemistry, Dalhousie University, Halifax, Nova Scotia B3H 4J3, Canada

Received 12 May 1995; revised 23 August 1995; accepted 23 August 1995

Abstract

A rotating, variable-wavelength interference filter has been used to acquire spectra from peak or baseline of a dual-channel, high-sensitivity flame photometric detector. On its spectral channel, the device monitors 100 data points from 400 to 700 nm ten times a second, and ensemble-averages them over seconds to (if needed) hours of acquisition time. The spectra can be smoothed, adjusted for background, corrected for filter transmission and photocathode profiles, and plotted with energy or photon ordinates. The extent of spectral fluctuation suggests the emergence of flicker noise at high analyte concentrations.

Keywords: Detectors, GC; Flame photometric detectors

1. Introduction[2]

The flame photometric detector (FPD) [1–6] has had a long and varied history. Soon after it became commercially available in single-channel form, it quickly developed into a dual-channel sensor: mainly to widen its immediate elemental range, but also to increase its chemical (spectral) information content (see e.g. Refs [7–12]). To maximize spectral information and to facilitate the task of selecting wavelengths for correlation (i.e. subtraction [13] or conditional-access [14,15]) chromatograms, we recently provided the FPD with a rotating variable interference filter plus dedicated electronic hardware and software. The setup produced ten simultaneous, wavelength-selective chromatograms. From the chromatograms of this "3-D FPD", crude 10-point spectra of peaks or baseline could be extracted by computer [16].

Yet, while gaining a new spectral dimension, the FPD lost some of its old sensitivity. The minimum detectable amounts that could be obtained from the filter wheel arrangement were typically an order of magnitude higher than those from a conventional FPD. At the same time, the spectral resolution was still much worse than that of the variable filter, owing to some compromises in optical, mechanical and electronic design [16]. Also, each spectral acquisition lasted less than one tenth of a second, with no direct provision made for integrating luminescent events over long time periods. The present study strives to eliminate these shortcomings.

*Corresponding author.

[1] Presented in part at the *Symposium on Environmental Chemistry, Dalhousie University, Halifax, Canada, October 1994.*

[2] Readers interested in a more comprehensive Introduction are invited to contact the corresponding author.

0021-9673/96/$15.00
SSDI 0021-9673(95)00926-4

2. Experimental

2.1. Optical layout

For this study, the same dual-channel Shimadzu GC-4BMPF that we had been using for more than twenty years was modified to accept a rotating variable interference filter on one side and a photomultiplier tube on the other. The filter and its housing were the same unit as used for the earlier 10-segment "3-D FPD" [16]. To recall briefly pertinent vendor's specifications (item no. 57496, Oriel Corporation, 250 Long Beach Blvd., Stratford, CT, USA): the semicircular filter covered the 400 to 700 nm wavelength range over 172 degrees at a dispersion of 1.75 nm/degree, with a 17-nm maximum bandpass and a 15% minimum transmission.

Fig. 1 shows a rough schematic representation of the mechanical and optical layout. The 6″×1/4″-diameter glass image conduit (Edmund Scientific Co., Barrington, NJ, USA; item no. 38307) was used with a ball lens of 10-mm diameter (Edmund no. 32748) held in a plastic tube. The two photomultipliers, which are not shown to scale, were an R-1104 multi-alkali PMT for the spectra collector and an R-268 or R-374 PMT for the holophotal channel (all PMTs were bought from Hamamatsu, Middlesex, NJ, USA). The mirror was roughly hemi-elliptical, with the flame situated at its focal point.

Alternatively, the image conduit was used with a 6-mm diameter planoconvex lens of 6-mm effective focal length (Edmund no. 45,078) to act as a collimator, and with the ball lens replaced by a short, black cylinder. This arrangement, which has a lower light throughput but produces a less divergent beam and hence a narrower bandpass, is shown at the bottom of Fig. 1.

2.2. Filter calibration

The spectral response from the filter-carrying wheel was defined in terms of wavelength and transmission. A flashlight bulb and a previously calibrated quarter-meter monochromator (Jarrell-Ash

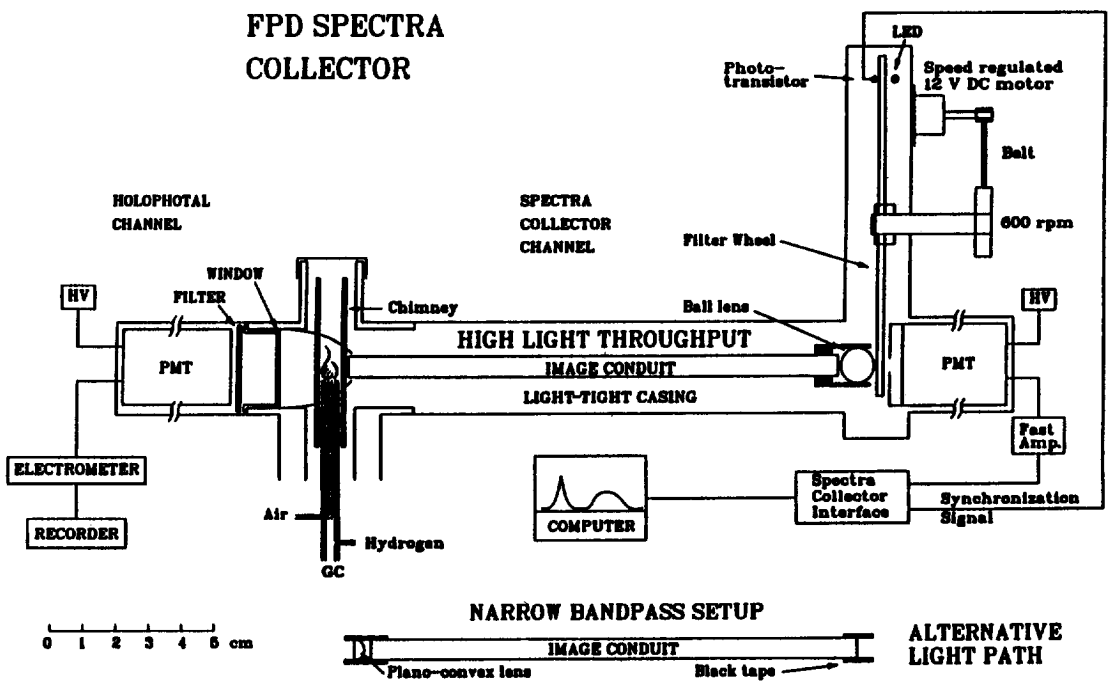

Fig. 1. Layout of chromatographic (left) and spectral (right) channels.

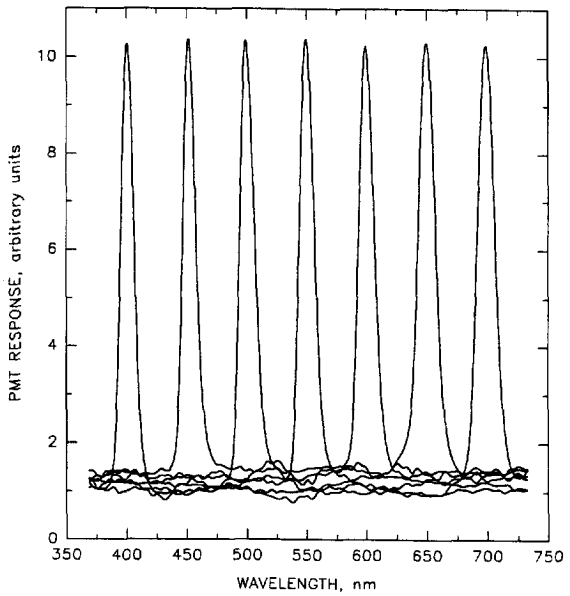

Fig. 2. Wavelength calibration of variable interference filter and spectra collector. Amplitudes are scaled to approximately the same value.

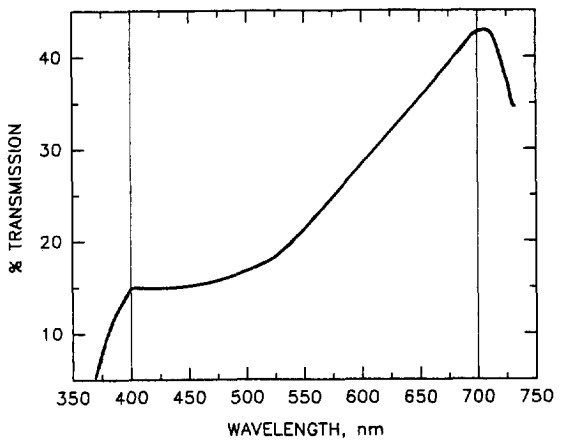

Fig. 3. Percent transmission characteristics of variable interference filter. The vertical lines mark the specified range of the filter.

Model 82-415 with a 1180 grooves/mm grating blazed for 500 nm and 0.5-mm slits) was used to ensure wavelength accuracy. Fig. 2 shows the superimposed records of seven beams (roughly adjusted to equal amplitude for this representation). The small deviations from the true wavelength were corrected by scaling the appropriate software parameters.

A similar arrangement was used, with the variable filter being moved into and out of the light beam, to measure the percent transmission profile shown in Fig. 3. While Fig. 2 and Fig. 3 are obviously valid only for a particular filter and instrumental set-up, they are included here for the sake of documentation. The percent transmission profile was used, together with the response profile of the photomultiplier tube (as taken from the Hamamatsu catalogue) to correct (rather roughly) the experimental signal intensities.

2.3. Data acquisition

The optical filter wheel assembly was the same unit that monitored the earlier 3-D FPD. Also, the earlier preamplifier (Fig. 1 in Ref. [16]) was used again; however, a 200-pf capacitor was removed from the PMT input to achieve the temporal resolution necessary for acquiring a larger number of samples (100 as compared to the earlier 10) per revolution of the wheel. There was nothing unusual about this circuit other than that it was housed in a small steel enclosure mounted close to the PMT, and that it was powered by an external 12-V a.c. adapter. This kept any stray a.c. fields from interfering with the sensitive input amplifier. For some concluding experiments, a similar arrangement but with a higher-quality amplifier (OPA 128 KM, Analog Devices, Norwood, MA, USA) was used to further depress electronic noise. The amplified signal was then forwarded to a newly designed data collection assembly.

The design of this assembly was influenced by two considerations. First, the data collection rate was ten times faster than that of the 3-D FPD. Second, the software was written in Visual Basic running under Windows 3.1. This required a dedicated microcontroller to circumvent the limitations of Windows 3.1 with respect to real-time operations. The microcontroller's role was to collect and sum – i.e., ensemble-average – the one hundred digitized data points per scan in 1.5-s packets of fifteen scans each, for transmission to the host computer. The electronic blueprint of this vital assembly is shown in Fig. 4.

The signal from the PMT preamplifier was introduced through pin 28 of J4, carrying one (negative)

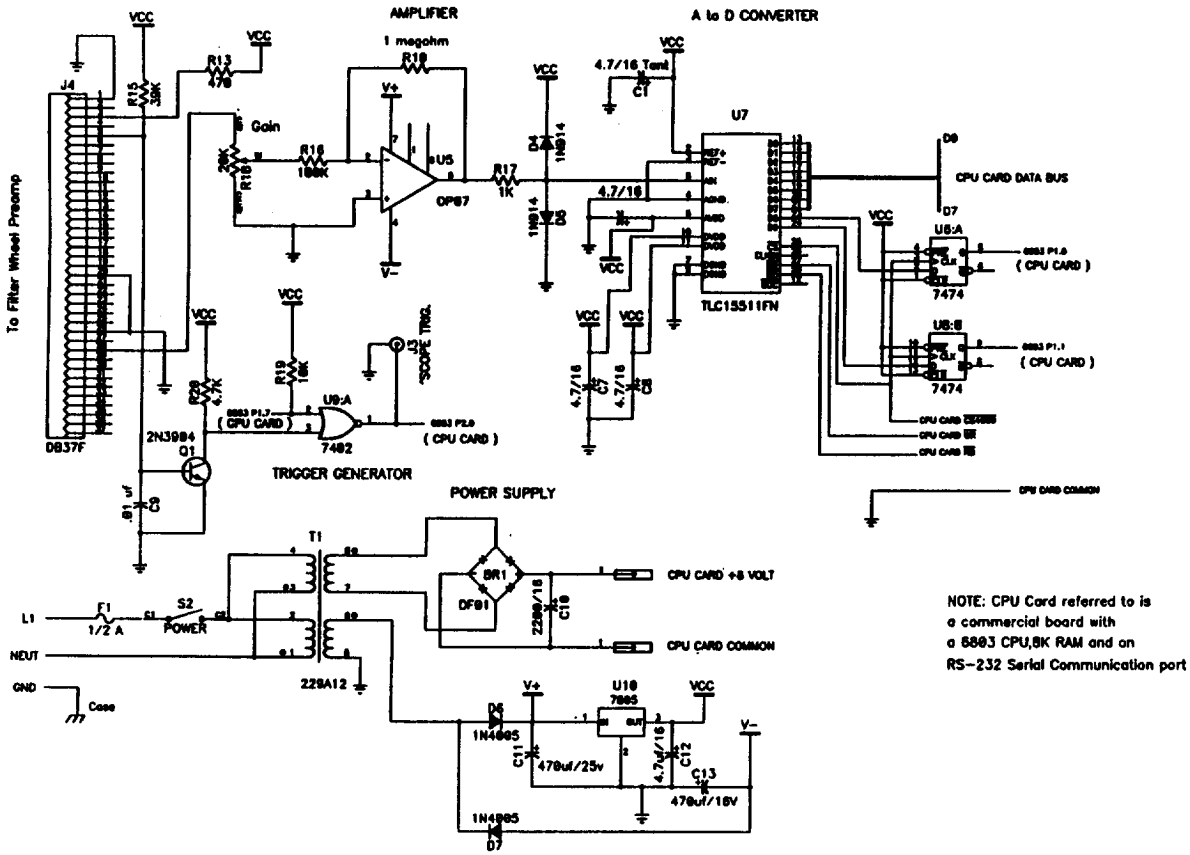

Fig. 4. Spectra collector electronic assembly. See text for explanation.

volt per one nanoampere of current (PMT plus bucking). After passing through the "gain" potentiometer R18, it was inverted and increased ten-fold by amplifier U5. The now positive signal was fed through a clamp circuit (R17, D4, D5) to prevent out-of-range voltages from damaging the input U7 to the TLC15511FN analog-to-digital converter (ADC).

The ADC had a resolution of 10 bits. That proved perfectly adequate for the low signal-to-noise ratio of the incoming signal. Because the ADC was a ten-bit unit feeding a microprocessor with a bus width of only 8 bits, a dual flip-flop (U6, U8) was used to latch the two most significant bits. These were read separately via two parallel-port lines of the microprocessor (P1.0 and P1.1).

As in the 3-D FPD [16], the data collection was synchronized with the filter rotation via an optical chopper mounted in the filter wheel assembly. (Its light-emitting diode was later shown to add some stray light to the signal, but this disturbance was too small to matter in the present context.) The optical chopper used the circuit surrounding Q1 and U9:A in Fig. 4. The role of the "OR" gate U9:A was to prevent chopper pulses from reaching the microprocessor port pin P2.0; this pin served a different purpose during the RESET process. The signal from P1.7, which fed U9:A, performed the gating chore.

The conventional full-wave bridge rectifier BR1 powered the separate CPU (central processing unit) card. Two half-wave rectifiers, D6 and D7, and the regulator U10 provided power for the analog functions and offered a separate 5-V source for the analog-to-digital converter. The performance of the latter was measurably improved by this well filtered and regulated power supply.

The microprocessor was based on a 6803 8-bit microcontroller mounted on a small circuit card. This card also contained the 2764 program EPROM, 8 K

of RAM memory, an RS-232 serial port, and a 5-V regulator plus negative power source for the RS-232 driver IC (integrated circuit). The schematic for this circuit has not been included in Fig. 4, since many commercial boards offer these features.

2.4. Data manipulation

Coming out of RESET, the 6803 microprocessor first determined the speed of the wheel's rotation by measuring the time difference between the rising and the falling edge of the signal from the optical chopper. It then conveyed the calculated speed value to the host computer, which put it on screen for operator's approval. Approval having been obtained, the microprocessor divided by one hundred the measured temporal interval between the rising and falling signal edges, and used the result as the sampling period for the rest of the experiment. This ensured that the one hundred samples taken during one revolution of the wheel were evenly spread throughout the optically active (transparent) portion of the variable interference filter.

Following this initial measurement the software remained in a loop, acquiring and averaging datapoints in packets of 15 for each of the 100 spectral samples, and sending them to the host computer via the RS-232 serial data link. Each download thus represented the ensemble sum of 15 spectra, acquired during 1.5 s of operation (for a wheel speed of 600 rpm). The data were transmitted by the microprocessor at 9600 baud and checked by the receiving computer for data integrity by "checksum" calculations performed on each 1.5-s transmission. Subsequent data manipulation and display were then handled by high-level programs in the host computer.

2.5. Spectral collection programs[3]

The spectra collector can run under two programs, depending on its experimental task. Program A is primarily designed for chromatographic and analytical scans of complex chromatograms, as well as for quick sample surveys; program B is primarily dedicated to spectra acquisition, correction and documentation, particularly if involving baselines, broad peaks, or continuous sample inputs.

Program A shows on the screen the current spectrum, as ensemble-averaged and displayed for 1.5 s. This provides the operator with continuously updated spectral snapshots of the analytes passing through the detector (and being simultaneously displayed as chromatographic peaks on the second channel). The spectral "baseline" (luminescent background) can be easily suppressed by a d.c. offset. The operator, if interested in a particular emerging peak or spectrum, can activate start and stop buttons, thereby committing a particular spectral section to memory. When recalled from memory, this section is displayed and/or printed as a normalized spectrum, i.e. with its highest intensity scaled to 100%.

Program A provides easy visual observation of developing complex chromatograms. It can also download a chosen spectrum directly to a printer via an RS-232 port, or export it in ASCII format into a spreadsheet-based program like Sigmaplot (Jandel Scientific, San Rafael, CA, USA). Program A is thus well suited to fast first runs, initial parameter adjustment, and the like.

In contrast, program B shows on the screen the integrated total (not the last acquired) ensemble-averaged spectrum. For this mode, the simultaneously available second-channel (chromatographic) readout is vital: it alone allows the operator to monitor events (e.g. emerging peaks, shifting baselines, etc.) and to activate accordingly the start/stop buttons for spectral documentation. During such recordings, the screen lists the number of "samples" (=1.5-s packets) so far summed, and shows the spectrum so far acquired. The latter display gives the operator the chance to judge the quality of the evolving spectrum, particularly its decreasing noise level. The program also keeps track of the absolute signal sums for all spectral data points. Similar to program A, spectra can be directly printed, and/or inserted into a spreadsheet for further manipulation.

2.6. Off-line spectral correction

If a peak is monitored, program B allows its spectrum and that of an equally long section of baseline to be imported into the spreadsheet. Thanks

[3] Researchers interested in these and other programs for non-commercial purposes are invited to contact B.M. for executable copies.

to the available absolute intensity values, the baseline spectrum can be deducted from the peak spectrum. Proper spectral deduction presumes, of course, that the baseline character did not change and that its amplitude did not drift; it also presumes that baseline and peak spectra were additive, i.e. amplitudinally independent of one another.

Other corrections or manipulations of the acquired spectra can be carried out on the spreadsheet, for instance correction for the wavelength dependence of the photomultiplier's response and the filter's light transmission. Also, the spectral intensity can be plotted as energy or number of photons, with the *y*-axis showing these scales (whose absolute values are not normally determined) as "percent of maximum".

3. Results and discussion

3.1. Performance of the chromatographic channel

The high-sensitivity chromatographic channel uses, to a large extent, the "holophotal" design described earlier [17,18]. It is not surprising, therefore, that similar performances were obtained for a variety of typical FPD analytes (S, P, Sn, Mn). However, precise analytical figures-of-merit were not again determined.

In contrast to earlier use of the variable filter wheel [16], the present arrangement includes a high-sensitivity FPD-type channel. This channel generally provides a higher light-throughput and hence a lower detection limit than does a conventional FPD [18]. It also allows a continuous comparison of wavelength-variable and wavelength-fixed signals.

3.2. Performance of the spectral channel

Compared to the earlier arrangement [16], the spectral channel offers not just snapshots of 10-point spectral envelopes, but 100-point spectra integrated over time intervals ranging from the unit packet of fifteen sequentially acquired and ensemble-summed scans to summations of hour-long luminescent events. (The longest "event" actually monitored lasted about 30 min.)

A major objective of the construction was to preserve the inherent bandpass of the variable filter. There are many reasons why the bandpass can widen: the flame is diffuse, the fibre optic with ball lens provides good light-throughput but poor focussing, the light rays cross the filter cavities at a fairly wide range of angles around the perpendicular, the aperture is relatively large, the filter rotates past the aperture at 600 rpm, and data manipulation makes frequent use of digital smoothing.

The top half of Fig. 5 shows the sodium resonance doublet at 589 nm from a Na-doped FPD-type flame. The bandpass is 16 nm, i.e. only marginally larger than the 15 nm measured for 600 nm light in Fig. 2. Its profile is slightly asymmetric, tailing toward the red. The profile was obtained with the "narrow-bandpass setup" shown at the bottom of Fig. 1. When the "high light-throughput" arrangement was used instead, the bandpass broadened to about 30 nm and the asymmetry became more pronounced.

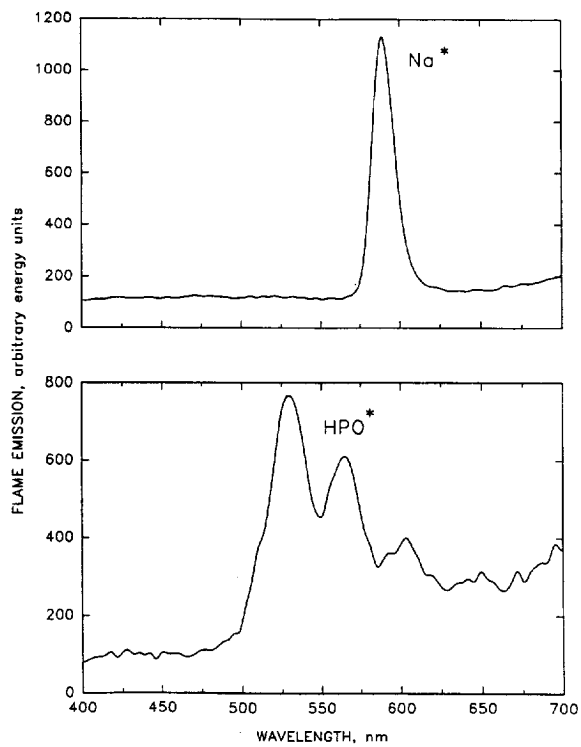

Fig. 5. Spectra from FPD flame doped with sodium (top, Program A) and tris(pentafluorophenyl)phosphine (bottom, Program B). "Narrow-bandpass setup" (see Fig. 1) used for acquisition. Data are corrected for PMT response and filter transmission, but are not smoothed.

This clearly indicates the major reason for the lower resolution. In the "high light-throughput" configuration, the beam enters the image conduit, and leaves it via the ball lens, in a highly divergent form. A ray of, say, 600 nm wavelength striking the filter at angles of incidence of 20° or 30° will appear in the spectrum shifted by about 1 or 3%, i.e. at about 606 or 618 nm, respectively. (Since the effective refractive index of the filter was not known, these numbers were determined experimentally.) The larger the fraction of light striking the filter at another than a right angle, and the greater the angle of incidence, the wider will be the bandpass and the more pronounced the tailing toward the red of the transmission profile.

Using a planoconvex lens to roughly collimate the light from the flame, and preventing its more divergent rays from reaching the filter, does indeed rectify the situation. On the other hand, the light throughput is dramatically lowered. As a consequence, and roughly in accordance with the square law for shot noise, the detection limit is degraded by about a factor of five. The lower half of Fig. 5 shows the spectrum of HPO* as obtained under these conditions from tris(pentafluorophenyl)phosphine. Some of the major bands, e.g. those at 525, 570 and 599 nm, are clearly visible.

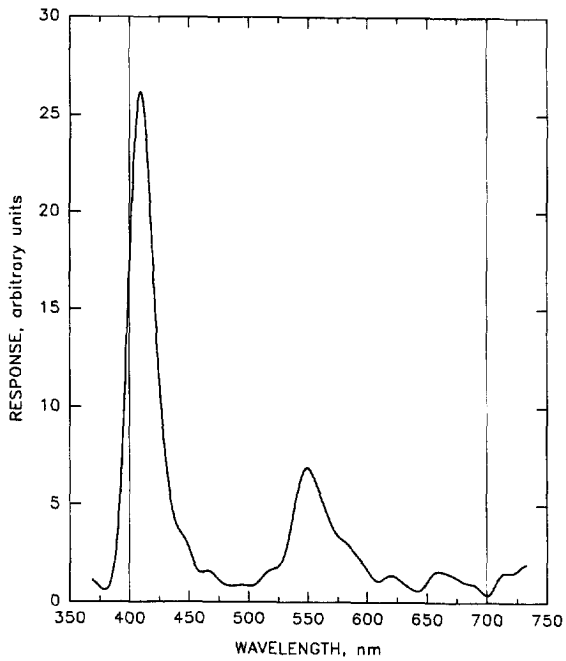

Fig. 6. Spectrum collected from a 0.8 μg peak of MMT, smoothed by four passes of a 3-point (ca. 10 nm) non-weighted moving average. Program A, "high light-throughput" arrangement (see Fig. 1).

In contrast, Fig. 6 provides the example of an atomic line measured in the "high light-throughput" configuration. The major peak at 403 nm represents the two resonance lines of the manganese atom, obtained here from a peak of the common antiknock compound MMT (methylcyclopentadienylmanganese tricarbonyl). Unsmoothed the bandwidth at half height was about 20 nm; typical digital smoothing widened it to about 25 nm.

3.3. Sundry spectra and spectral readouts

In addition to sodium, phosphorus and manganese, the typical FPD analyte elements sulfur and tin were tested and produced their well-known spectra from conventional peaks. There was no mistaking their identity as they appeared on the screen as 1.5-s peak slices in the "Program A" mode, hence they are not shown here.

In greater need of illustration was the "Program B" mode – not just for passing peaks (for which, guided by the chromatographic channel, it worked well), but for continuously introduced analyte. Either organosulfur or organophosphorus compounds were doped into the hydrogen supply line from headspace generated in a thermostatted bath. While the resulting spectra brought no surprises, it is interesting to display the "after-effect" of these measurements. As FPD operators are only too well aware, sulfur and phosphorus compounds tend to sorb in the chromatographic system and elute only very slowly. In other words, the FPD baseline (the luminescent background) often reflects sample history.

Since memory effects of this nature can severely degrade analytical performance, spectra of the baseline become valuable diagnostic tools. As a demonstration, Fig. 7 shows the spectra of essentially constant levels of phosphorus and sulfur species – obtained long after the doping streams of organophosphate and sulfone had been shut off. As expected, the S_2 bands are too close to be resolved, but there is little doubt about their identity or that of the HPO bands. Fig. 7 actually shows the overlay of

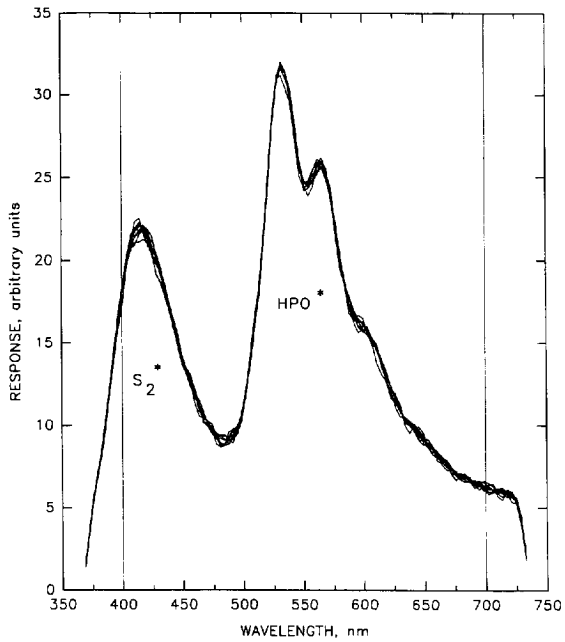

Fig. 7. Vapour from tubes previously exposed to phenylsulfone and triethylphosphate. Raw-data overlay of nine sequential 1-min spectra obtained by Program B (no spectral correction, no smoothing).

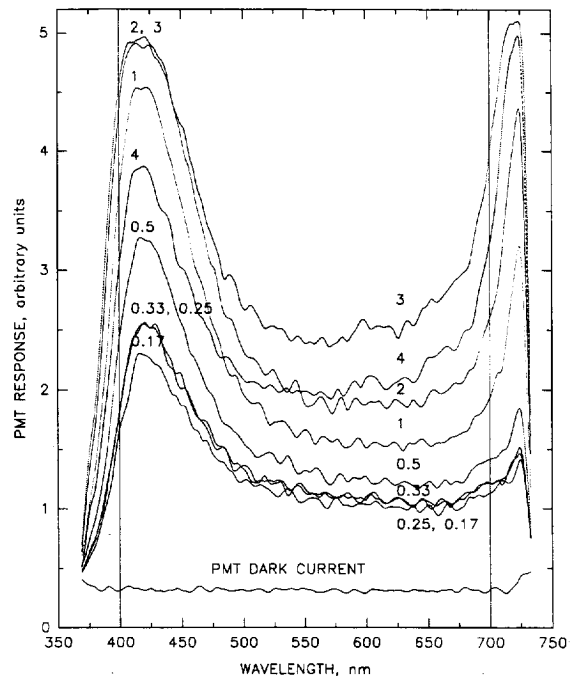

Fig. 8. Luminescent background of "clean" FPD flames of different air/hydrogen ratios (as marked on curves). Acquisition time 75 s each. Conditions in ml/min of air/hydrogen: 200/50, 150/50, 100/50, 50/50, 50/100, 50/150, 50/200, 50/300. Overlay of raw data (no spectral correction, no smoothing).

nine sequential 1-min spectral collections, thereby documenting the tenacious nature of the memory effect and the excellent reproducibility of the spectra.

Of course, this is primarily a demonstration experiment. Yet, even with a fairly clean system (including a new quartz chimney), the background luminescence still shows significant spectral features. With the installation of the wheel [16] it became easy to measure these features for different flows of hydrogen and air [19]. Typically, high hydrogen/air ratios produced emission that was predominantly in the blue and relatively weak; low hydrogen/air ratios (but generally still within a hydrogen-rich range) produced emission that was predominantly in the red and relatively strong. Some of the 10-point spectra from differently constituted flames thus crossed each other [19].

For the present purpose, a similar experiment was again run. Fig. 8 shows the raw (i.e. neither smoothed nor corrected) data for eight air/hydrogen volume ratios from hydrogen-rich to air-rich (the ratio of the stoichiometric flame is, of course, 2.5). The spectra were collected for 75 s each. The fluctuation that shows up in the middle section of the wavelength range is mere noise.

With moderate smoothing, corrections for the percent transmission of the wheel and the response profile of the photomultiplier tube, and conversion of the intensity axis from energy to photon flux, Fig. 9 emerges. By itself it is of little importance – baseline features are notoriously fickle – but its appearance demonstrates well the effects of spectral manipulation. The reason that the emission now appears so much stronger in the red is the sharply declining PMT response profile and the change of ordinate units from radiant energy to number of photons.

3.4. Minimum spectral noise

It is interesting to determine the minimum (i.e. quantum) fluctuations of a spectral trace. This unavoidable noise component is easily estimated from counting statistics as the square root of the smallest

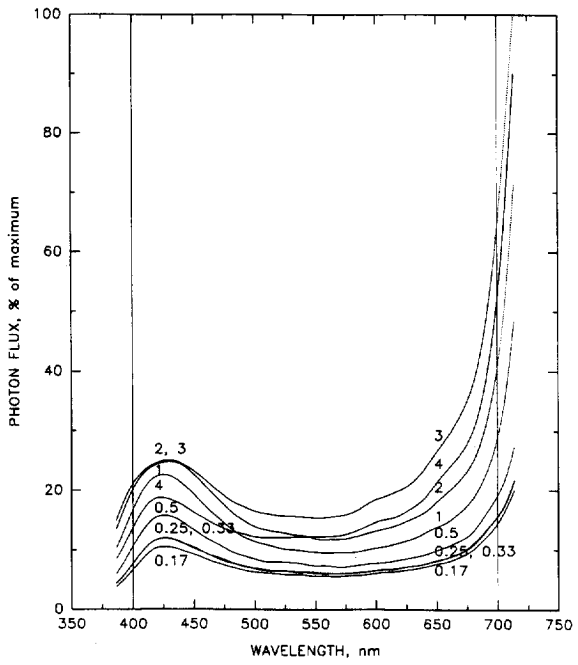

Fig. 9. Photon flux from "clean" FPD flames of different air/hydrogen ratios as in Fig. 8. Data corrected for interference filter transmission and photocathode responsivity profiles. Smoothing by three passes of a 3-point (about 10 nm) moving window.

rate in signal transmission, in this case the generation of photoelectrons from the PMT's light-sensitive cathode (cf. [20]). The rate of photoelectron generation can be experimentally determined for a particular datapoint by keeping the filter stationary at that wavelength and measuring the current.

The signal S of interest, i.e. the number of photoelectrons generated for that datapoint, is then:

$$S = \frac{I \times d}{e \times g}$$

where I is the (total) measured current in amperes, e is the charge of the electron (1.6×10^{-19} As), g is the gain (electron multiplication factor) at the chosen PMT voltage, and d is the total dwell time on that wavelength segment (identical with the acquisition time t for a stationary wheel).

During regular spectral acquisition, where the wheel (representing a semicircular array of 100 wavelength segments) completes ten rotations per second, the total dwell time for one segment is:

$$d = 5 \times 10^{-3} t$$

If the spectrum is smoothed by a window or boxcar algorithm over a width of w data points, the approximate time frame becomes:

$$d = 5 \times 10^{-3} t \times w$$

For it

$$S = \frac{I \times 5 \times 10^{-3} t \times w}{e \times g}$$

and its fundamental noise N, expressed as the standard deviation of the signal, is $S^{1/2}$. The most practical noise definition for a spectrum would seem to be the peak-to-peak or the ±%R.S.D. band. The width of the latter at the chosen data point (wavelength) is:

$$\%\text{R.S.D.} = \pm\frac{100\,N}{S} = \pm 100\sqrt{\frac{e \times g}{I \times 5 \times 10^{-3} t \times w}}$$

A fairly typical example: for a current of 10^{-7} A, a total acquisition time of 10 s, and a 3-point window used for smoothing, R.S.D.=±0.03%.

In repeated measurements of smaller and larger, sharper and broader peaks, it soon became clear that the measured signal variation was usually significantly larger than the one calculated by assuming quantum noise only. Though unwelcome, this was not overly surprising: emission in "spectroscopic" flames is known to shift from fundamental to multiplicative with increasing levels of analyte [21].

While the noise important in chromatography is that of the baseline, here, as well as in most of spectroscopy, it is that of the signal (including the baseline). In the current experiments, typical spectral noise bands were about 2 to 5 times wider than calculated for fundamental noise alone. While this hardly matters for chromatographic quantitation, it does limit spectral interpretation. Under favourable circumstances, multiplicative noise can be reduced by instrumental means. An investigation of the particular character and reduction of noise in the described system is, however, beyond the confines of the present study: it will be given at another time.

Acknowledgments

This study would not have been possible without the extraordinary machining skills and exemplary

cooperation of C.G. Eisener, and without the financial support of an NSERC Individual Research Grant.

References

[1] M. Dressler, Selective Gas Chromatographic Detectors, J. Chromatogr. Library, Vol. 36, Elsevier, Amsterdam, 1986, pp. 152–156.
[2] S.O. Farwell and C.J. Barinaga, J. Chromatogr. Sci., 24 (1986) 483.
[3] E.R. Adlard, CRC Crit. Rev. Anal. Chem., 5 (1975) 13.
[4] S. Kapila, K.O. Duebelbeis, S.E. Manahan and T.E. Clevenger, in R.M. Harrison and S. Rapsomanikis (Editors), Environmental Analysis Using Chromatography Interfaced with Atomic Spectroscopy, Ellis Horwood, Chichester, 1989, Ch. 3.
[5] P.T. Gilbert, in R. Mavrodineanu (Editor), Analytical Flame Spectroscopy, Philips Technical Library/Macmillan, London, 1970.
[6] S.S. Brody and J.E. Chaney, J. Gas Chromatogr., 4 (1966) 42.
[7] M.C. Bowman and M. Beroza, Anal. Chem., 40 (1968) 1449.
[8] V.A. Joonson and E.P. Loog, J. Chromatogr., 120 (1976) 285.
[9] A.R. Baig, C.J. Cowper and P.A. Gibbons, Chromatographia, 16 (1982) 297.
[10] R.S. Braman, Anal. Chem., 38 (1966) 734.
[11] W.A. Aue and H.H. Hill, Anal. Chem., 45 (1973) 729.
[12] D.A. Leathard and B.D. Shurlock, Identification Techniques in Gas Chromatography, Wiley, London, 1970, particularly Ch. 8.
[13] W.A. Aue, B. Millier and X.-Y. Sun, Can. J. Chem., 70 (1992) 1143.
[14] W.A. Aue, B. Millier and X.-Y. Sun, Anal. Chem., 63 (1991) 2951.
[15] W.A. Aue, X.-Y. Sun and B. Millier, J. Chromatogr., 606 (1992) 73.
[16] B. Millier, X.-Y. Sun and W.A. Aue, J. Chromatogr. A, 675 (1994) 155.
[17] W.A. Aue, C.G. Eisener, J.A. Gebhardt and N.B. Lowery, J. Chromatogr. A, 688 (1994) 153.
[18] W.A. Aue, C.G. Eisener, J.A. Gebhardt and N.B. Lowery, J. Chromatogr. A, 699 (1995) 195.
[19] X.-Y. Sun, unpublished research, Dalhousie University, 1993.
[20] W.A. Aue, H. Singh and X.-Y. Sun, J. Chromatogr. A, 687 (1994) 283.
[21] C.T.J. Alkemade, W. Snelleman, G.D. Boutilier and J.D. Winefordner, Spectrochim. Acta, 35B (1980) 261.